JOURNAL OF CATALYSIS 88, 466–477 (1984)

An X-Ray Photoelectron Spectroscopy and Reaction Study of Pt–Sn Catalysts

B. A. SEXTON, A. E. HUGHES, AND K. FOGER

CSIRO Division of Materials Science, Catalysis and Surface Science Laboratory, University of Melbourne, Parkville, Victoria, 3052, Australia

Received October 6, 1983; revised March 20, 1984

Platinum–tin catalysts prepared by different methods, and supported on γ-Al_2O_3 have been studied with X-ray Photoelectron Spectroscopy (XPS), temperature-programmed reduction, and reaction measurements. Two major conclusions are drawn from the results. First, tin is present primarily in the oxidized form (Sn(II)) after high-temperature reduction (500°C) of Pt–Sn/γ-Al_2O_3 catalysts, whereas alloy formation can occur on silica under the same conditions. No evidence for substantial amounts of Sn(0) is found on reduced γ-Al_2O_3-based catalysts. The spectroscopic reduction results are in agreement with TPR measurements in the present (and previous) work which show an average Sn reduction of 50%. Even Pt–Sn complexes, which are readily reducible to Sn(0), are not reduced below Sn(II) on γ-Al_2O_3. Second, quantitative XPS measurements of surface tin concentration versus bulk loading reveal an inhomogeneous distribution of tin in the impregnated γ-Al_2O_3 samples, with a large excess of tin on the external surface of Al_2O_3 at loadings below 1 wt% Sn. The results show that impregnation of tin followed by platinum can result in separation of the two components due to the strong adsorption of tin ions in the outer surface of the γ-Al_2O_3 particles. The best distribution of tin is found in the coprecipitated Sn–γ-Al_2O_3 (Patent) preparations where the tin is uniformly distributed throughout the matrix. The reaction measurements of catalysts prepared via the different methods are compared and it was concluded that the activities and selectivities in methylcyclopentane and cyclohexane conversion are sensitive to the method of tin introduction. A catalyst prepared via the coprecipitation of Sn with γ-Al_2O_3 followed by impregnation of platinum gave the highest sensitivities to activity and selectivity changes in the latter reactions. Whereas it is important to have platinum and Sn(II) in the vicinity of each other on the support, the mechanism of interaction is not well understood at this stage.

INTRODUCTION

Recent studies of platinum–tin/γ-Al_2O_3 catalysts have debated the chemical state of tin species present after high-temperature reduction. Burch (*1*) claimed from temperature-programmed reduction measurements that the average oxidation state of Sn was Sn(II) and was independent of the Sn concentration over the range 0.3 to 5 wt% Sn. Burch's work implied that no significant amounts of Pt–Sn alloys were formed on γ-Al_2O_3-based catalysts and that the Sn(II) species were adsorbed primarily on the alumina. These results are in conflict with earlier work by Dautzenberg *et al.* (DHBS) (*2*) who concluded that the first 0.6% of tin present on the catalyst was in the oxidized form ("chemically complexed by the alumina") but higher loadings in excess of this value were reduced to metallic tin. DHBS were only able to detect Pt–Sn alloy formation after reduction for 100 h at 650°C, however. They noted that Pt–Sn alloys were easily observed on silica-supported catalysts after reduction at 350°C. Muller *et al.* (*3*) concluded from earlier hydrogen–oxygen titration experiments that the lowest oxidation state of tin was Sn(II) on γ-Al_2O_3 catalysts up to 1.4% Sn. Bacaud *et al.* (*4*) claim to have detected Pt–Sn alloy formation on low-loading Pt–Sn/Al_2O_3 catalysts with Mössbauer spectroscopy, as well as Sn(IV) and Sn(II) ionic species after reduction for 1 h at 500°C.

There have been very few X-ray photoelectron spectroscopic measurements of supported Pt–Sn/γ-Al_2O_3 or silica cata-

0021-9517/84 $3.00

lysts. Bouwman *et al.* (*5*) have measured Auger surface compositions of Pt/Sn alloys, and XPS and reaction data on γ-Al_2O_3-based catalysts has been discussed by Yermakov *et al.* (*6, 7, 10*) in several papers on catalysis by supported Pt–Sn complexes. Yermakov *et al.* have found that (Sn + Pt) complexes impregnated on γ-Al_2O_3 do not form alloys after reduction as determined by XPS, although alloys (or metallic Sn) were seen on SiO_2-supported catalysts. On γ-Al_2O_3 only Sn(II) or Sn(IV) species were found to be present after reduction.

In the present work we have attempted to resolve the dispute over the nature of tin present on γ-Al_2O_3 catalysts after reduction in the presence of Pt by using XPS, supported by both TPR and reaction measurements. Our results support the conclusion of Burch, Muller, and Yermakov, since we find that tin is not reduced below Sn(II) on γ-Al_2O_3-based catalysts for a wide range of preparations. We demonstrate that Pt–Sn alloys are formed on SiO_2 supports (TPR and XPS) in agreement with previous work.

Two aspects of the present work are significant. We use an *in-situ* high-pressure reduction cell to eliminate air exposure in the XPS experiments to demonstrate that Sn is not reduced below Sn(II) on γ-Al_2O_3 supports. This result is independent of the mode of tin introduction. Second, we quantitatively analyze the Sn/O surface ratios for all our catalysts and demonstrate that tin is present in surface excess with respect to the internal pores on the alumina matrix if normal acetone or aqueous impregnations are used. The reaction data complements the XPS data by measuring the overall degree of interaction between platinum and tin throughout the catalyst.

The XPS or reaction results do not rule out the formation of a dilute Pt–Sn alloy or Sn ions adsorbed on Pt particles. However, it is clear that γ-Al_2O_3-based Pt–Sn(II) catalysts should not be considered as a simple bimetallic system. We agree with Burch (*1*) that tin strongly adsorbs on the alumina and may act more as a surface modifier of alumina or as an electronic promoter (metal–support interaction) than as an alloying component.

EXPERIMENTAL

Five different catalyst preparations were used in the present work. In all preparations involving impregnation of γ-Al_2O_3 with tin salts, the tin was impregnated first, followed by impregnation of 0.5 wt% Pt (as H_2PtCl_6) after calcination at 500°C in air overnight. Experimental procedures were as follows: γ-Al_2O_3 (Akzo Chemie Grade ES, 125 m^2/g) was impregnated with tin by three different methods. Tin metal was dissolved in aqua regia to form an acidic solution, $SnCl_4 \cdot 5H_2O$ was dissolved in acetone and $SnCl_4 \cdot 5H_2O$ was dissolved in water (1% solutions) and then impregnated followed by evaporation to dryness and calcination to 500°C in air overnight. A range of catalysts was prepared with the tin content ranging from 0.2 to 6.3 wt%. Platinum was then impregnated (as H_2PtCl_6) on all the catalysts to a loading of 0.5 wt%. In the fourth preparation $[Pt(SnCl_3)_2Cl_2][Et_4N]_2$ was dissolved in acetone and impregnated onto γ-Al_2O_3 to a loading of 2.4 wt% Sn. Finally, a patented Pt–Sn catalyst was prepared by a coprecipitation method (U.S. Patent 4,032,434) in which tin ions are highly dispersed throughout the alumina matrix. Platinum (0.5 wt%) was impregnated into this catalyst by the normal method (aqueous H_2PtCl_6). All catalysts were subject to XPS measurements, temperature-programmed reduction, and reaction measurements, with some additional X-ray diffraction applied to selected samples.

For the XPS experiment, catalysts were pressed into 1.0-cm disks (~0.5 mm thick) and mounted on nickel-plated copper sample holders in a VG ESCALAB system. The catalysts were either unreduced or prereduced in a separate reactor at 500°C for 2–3 h. Prior to analysis, reduction of the samples was usually carried out in static

hydrogen (0.5 atm) in a high-pressure cell inside the ESCALAB preparation chamber. No difference in the XPS results was noted for samples which had undergone long prereduction at 500°C and samples which were initially reduced for only 10–30 min in H_2 prior to examination. XPS data was taken with Al$K\alpha$ radiation (100 W), at approximately 1.5 eV resolution (peak half-width) and signal averaging times of 4–80 min depending on the loading. Reference binding energies were Al 2*p* 74.3 eV and Si 2*p* 103.4 eV which gave values for Sn^0 and Sn(II, IV) of 484.8 and 486.6 eV, respectively. As pointed out by Lau and Wertheim (*8*) one cannot distinguish between Sn(II) and Sn(IV) in XPS because their binding energy difference is too small. The surface Sn/O ratios were calculated from the relationship

$$\left[\frac{\text{Sn}}{\text{O}}\right]_{\text{surface}} = 0.117\left[\frac{I\ \text{Sn}\ 3d}{I\ \text{O}\ 1s}\right]$$

where I is the integrated areas of the Sn 3*d* and O 1*s* lines. The multiplying factor is the inverse ratio of the cross sections, and the mean free path and transmission function factors are unity due to the close proximity of Sn 3*d* and O 1*s* in kinetic energy. In all of the quantitative studies, a calculated line of the expected Sn/O surface ratio versus wt% Sn based on 100% distribution of the Sn is included (*11*). We expect that the maximum error in any Sn/O results is $<\pm 10\%$. Analysis of the Pt 4*f* levels was not possible with any certainty because of overlap problems with the Al 2*p* line, and no Pt XPS data is included in the present discussion.

Temperature-programmed reduction (TPR) of the Pt–Sn/γ-Al_2O_3 catalysts was carried out in a once-through 5% H_2/N_2 stream at 0.33 ml · sec^{-1}. The sample size was 100 mg and the programming range 300–825 K. After subtracting the hydrogen consumed by reduction of platinum (which is assumed to be completely reduced to the metal), estimates were made of the average percentage reduction of tin to the metallic state. In addition, X-Ray Diffraction (XRD) and electron microscopy analyses were also taken on selected samples.

The conversions of MCP (methylcyclopentane) and CH (cyclohexane) were carried out in a flow reactor in the temperature range 570–670 K at a total pressure of 101 kPa. The reaction mixture contained hydrogen and hydrocarbon in a molar ratio of 8/1. The products were analyzed by gas chromatography using a 6-mm-packed OV-101 column and a FID detector. Prior to reactions the catalysts were treated under a flow of hydrogen at 670 K for 15 h.

RESULTS AND DISCUSSION

1. Temperature-Programmed Reduction Results

Temperature-programmed reduction curves were taken for most of the catalysts. For the sake of brevity we present the results for the tin/aqua regia and $SnCl_4 \cdot 5H_2O$/acetone series in Figs. 1 and 2. Each diagram has two series of curves, the upper curves for reduction of impregnated tin only, and the lower curve for impregnation of tin followed by 0.5 wt% Pt.

In general, the curves are similar for both series, with both tin preparations showing reduction commencing at 400–500 K and exhibiting a broad maximum near 700–800 K. High loadings (5–6 wt%) produced a second maximum near 500 K in the acetone series and a broad low-temperature tail for the aqua regia. After impregnation with platinum, both sets of profiles changed dramatically with a new sharp peak appearing near 520–570 K, and smaller maxima in the range 650–850 K.

Our TPR results are essentially in agreement with data obtained by Burch (*1*). The appearance of the sharp peak near 250°C (520 K) in Figs. 1 and 2 in the Pt–Sn catalyst spectra must be associated with reduction of platinum. Burch (*1*) has shown that monometallic Pt/alumina catalysts display a sharp reduction maximum near 520 K (250°C) for the uncalcined forms. Burch's

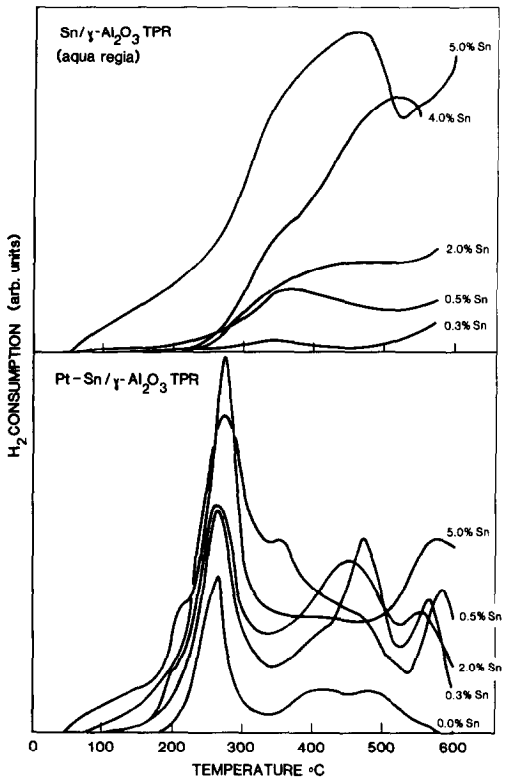

FIG. 1. Temperature-programmed reduction (TPR) profiles for Sn (upper) and Pt–Sn (lower) catalysts prepared by impregnating an acidic solution of Sn dissolved in aqua regia into γ-Al_2O_3. The loading of Pt was 0.5 wt%.

data indicated greater than 100% reduction of platinum assuming Pt(IV)–Pt(0) with the excess reduction being attributed to chlorine removal. We assume in the present work, as did Burch (*1*), that Pt(IV) is completely reduced to Pt(0). We calculated the percentage reduction of the tin in all of the series of catalysts prepared, after subtracting the contribution for the (Pt(IV)–Pt(0)) reaction. Our average result indicated that the degree of reduction of tin based on a Sn(IV) to Sn(0) reaction was 50 ± 10% and was not increased by the presence of platinum. The "average" oxidation state should therefore be Sn(II)-based on the TPR data. An "average" oxidation state of Sn(II) could include a metallic component, however, and it is important to examine the catalysts with XPS to differentiate between metallic and oxidized tin.

2. *XPS Analyses*

Two aspects of the surface properties of the Pt–Sn catalysts were examined with XPS. We measured the Sn 3*d* binding energies with respect to the Al 2*p* reference peak at 74.3 eV to determine the oxidation states present, and quantitatively integrated the Sn 3*d* and O 1*s* peak areas on a computer to determine the Sn/O surface atomic ratio. We have assumed in this work that the Pt is in the metallic state after reduction. Observation of the Pt 4*f* levels was not attempted due to the overlap problem with the Al 2*p* line of the substrate. We assume that platinum is completely reduced at the temperatures used in this study.

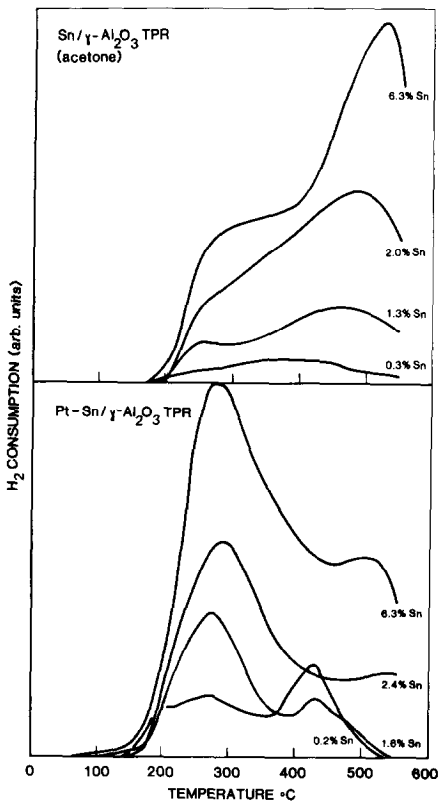

FIG. 2. Temperature-programmed reduction (TPR) profiles for Sn (upper) and Pt–Sn (lower) catalysts prepared by impregnating an acetone solution of $SnCl_4$ $5H_2O$ into γ-Al_2O_3. The loading of Pt was 0.5 wt%.

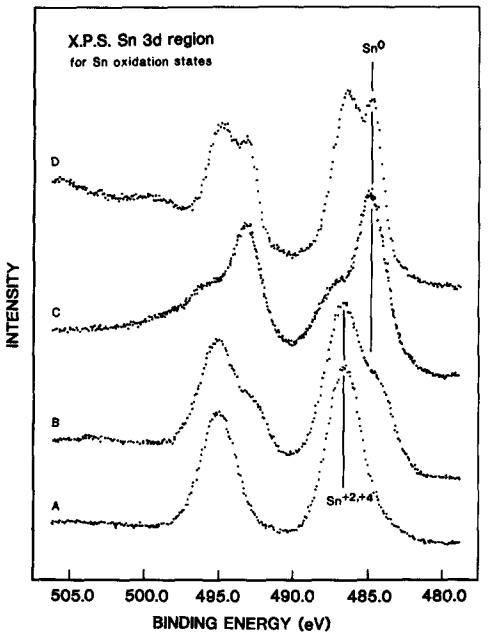

FIG. 3. Reference Sn 3*d* spectra showing both Sn(II,IV) lines and Sn(0). Curves A–C are supported SnO_2 exposed to increasing degrees of reduction, with (B) an ion beam and (C) atomic hydrogen. Curve (D) is air-exposed tin foil with a passive overlayer. These spectra provide line positions for Sn(0) and Sn(II,IV).

(*a*) *Determination of tin oxidation states.* As pointed out by Lau and Wertheim (*8*), there is approximately a 1.7-eV chemical shift between Sn(0) and Sn(II,IV) in the 3*d* spectra of oxidized tin, but one is unable to separate Sn(II) and Sn(IV) in XPS analyses. We examined reference samples which contained surface Sn(0), Sn(II), and Sn(IV) and the results are shown in Fig. 3. For the metallic tin 3*d* 5/2 line we obtained a binding energy of 484.8 ± 0.1 eV and for Sn(II,IV), 486.6 ± 0.1 eV. In Fig. 3, curve D is a piece of metallic tin with an air-formed passive layer which contains hydroxides and other oxides. We therefore take only the Sn(0) position from this curve. For curves A–C, Sn(IV) was supported on γ-Al_2O_3 to a loading of 3 wt% and subjected to increasing degrees of reduction. These samples were the most poorly dispersed of the Sn/aqua regia samples and differed from the rest of the preparations in that they contained some bulk phase of SnO_2 or SnO dispersed on the alumina (as determined by electron microscopy). Curve A is after reduction in hydrogen at 500°C, curve B after sputtering with an Ar^+ ion beam and curve C after exposing the sample to atomic hydrogen from a hot tungsten filament. These curves merely illustrate the changing shape of the spectra as the percentage of reduction increases.

With metallic tin present the shoulder at 484.8 eV increases in intensity at the expense of the 486.6-eV line. We estimate that at least 5% of the total tin would have to be in the metallic state for a positive identification of this state to be made.

All five series of catalysts (aqueous impregnated, aqua regia-impregnated, acetone, coprecipitated, and Pt–Sn complex) were examined with XPS before and after reduction at 500°C in static hydrogen in the high-pressure chamber attached to the ESCALAB. Reduction times were 10–30 min, and some samples were prereduced for several hours in a separate reactor under a flow of hydrogen, passivated in oxygen in the reactor then transferred to the ESCALAB for a short reduction to eliminate the effects of passivation and air exposure. As a general observation, *no* reduction of Sn(II,IV) to the metallic state was observed on *any* of the γ-Al_2O_3 samples for loadings ranging from 0.3 to 6 wt% Sn. Representative data is shown in Fig. 4 for the acetone-impregnated and coprecipitated catalyst. For the acetone case identical spectra are obtained before and after reduction indicating a lowest possible oxidation state of Sn(II). No evidence for metallic tin (>5% total) can be seen. The coprecipitated catalyst had a similar result although the signal-to-noise ratio was lower due to a better distribution of tin in these catalysts. Whereas the results in Fig. 4 are for Pt–Sn catalysts we observed no reduction below Sn(II) for catalyst samples which contained only tin.

As a further demonstration of the inability of Sn to reduce below Sn(II) on γ-Al_2O_3 we show data in Fig. 5 for the complex

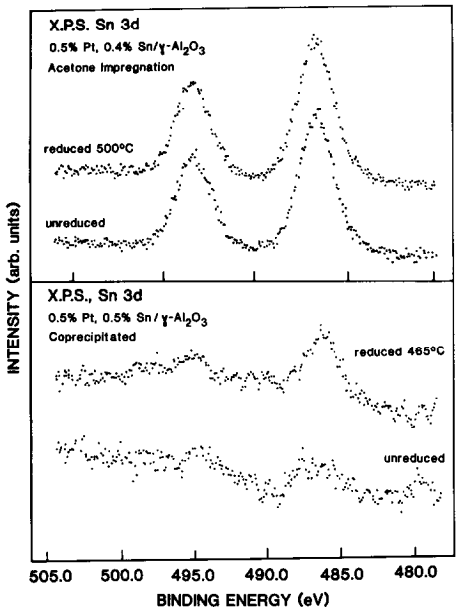

FIG. 4. Representative Sn 3*d* XPS spectra of catalysts before and after reduction. The upper catalyst is an acetone-impregnated Pt–Sn catalyst. The lower catalyst is a coprecipitated Sn–γ-Al_2O_3 catalyst with 0.5 wt% of Pt and Sn. Both spectra show only Sn(II) lines with no evidence for Sn(0) after reduction. The poor signal-to-noise ratio in the coprecipitated catalyst is caused by the better distribution of Sn in the bulk.

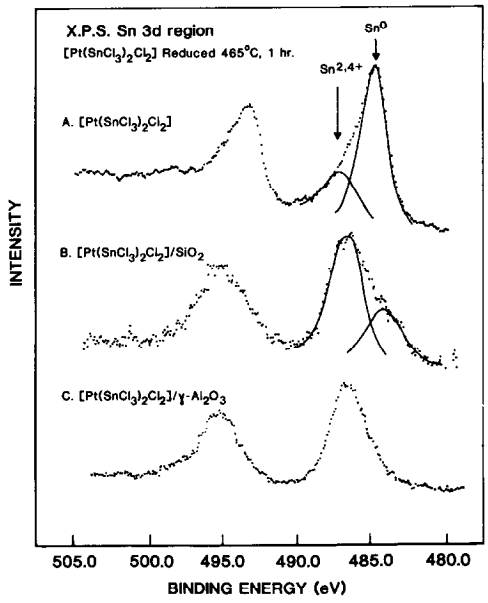

FIG. 5. Reduction of the complex $[Pt(SnCl_3)_2Cl_2][Et_4N]_2$. Curve A is the unsupported complex, curve B is supported on silica (2.4 wt% Sn), and curve C is supported on γ-Al_2O_3 (2.4 wt% Sn). Both A and B show significant reduction to Sn(0), whereas the γ-Al_2O_3-supported complex does not (curve C).

$[Pt(SnCl_3)_2Cl_2][Et_4N]_2$ supported on silica and supported on Al_2O_3 after reduction in hydrogen at 465°C for 1 h. We found that both tin and platinum reduced easily to the metallic state in the unsupported complex (curve A, Fig. 5). Tin, however, was only 30% reduced to Sn(0) on a silica support, and did not reduce below Sn(II) when supported on γ-Al_2O_3 (Fig. 5c). The silica case will be discussed later. Curve C in Fig. 5 gives further support to the idea that Sn(II) is the major oxidation state present after reduction of Pt–Sn/γ-Al_2O_3, and that there must be a strong reaction between Sn(II) and the γ-Al_2O_3 surface to prevent reduction of an otherwise reducible species (Fig. 5, curve A).

(*b*) *Quantitative determination of surface Sn/O ratios*. Quantification of the elemental ratios of Sn/O is possible by integration of the XPS Sn 3*d* (5/2 and 3/2 peaks) and O 1*s*

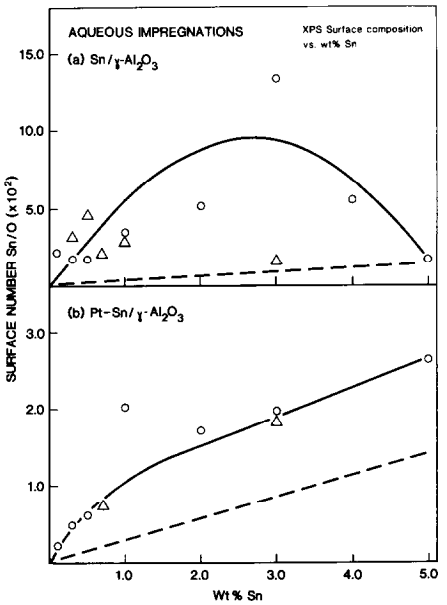

FIG. 6. The surface Sn/O ratio versus bulk composition (wt% Sn) for aqueous impregnations/γ-Al_2O_3. (○) Sn dissolved in aqua regia, (△) aqueous $SnCl_4 \cdot 5H_2O$. The dashed line is a theoretical line which assumes complete distribution of Sn throughout the γ-Al_2O_3 matrix.

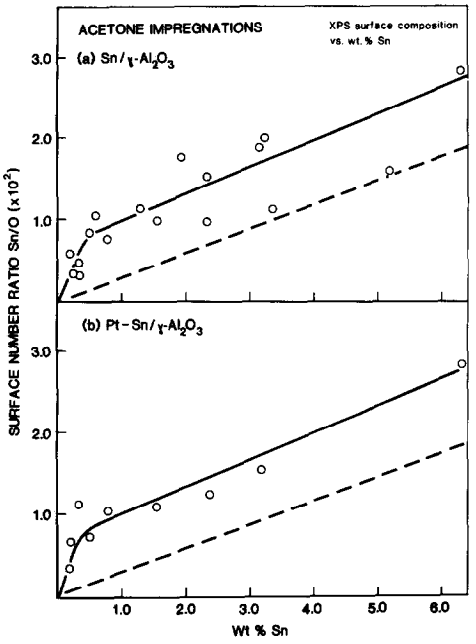

FIG. 7. The surface Sn/O ratio versus bulk composition (wt% Sn) for acetone impregnations/γ-Al_2O_3. The dashed line is a theoretical line which assumes complete distribution of Sn throughout the γ-Al_2O_3 matrix.

peak areas. The surface atomic number ratio Sn/O has been measured for each set of catalysts after reduction and the results are shown in Figs. 6, 7, and 8. Figure 6 refers to aqueous impregnation where $SnCl_4 \cdot 5H_2O$/water (triangles) and Sn dissolved in aqua regia (circles) were studied. Two curves are shown, for tin alone (upper curve) and after Pt impregnation (lower). A similar set of curves is provided in Fig. 7 for $SnCl_4 \cdot 5H_2O$/acetone impregnation. In Fig. 8 data for all of the reduced Pt–Sn catalysts are included in a single plot including the coprecipitated (Patent) preparations and the Pt–Sn complex. Each graph is a plot of surface number ratio (Sn/O) versus wt% Sn. The dashed line in Figs. 6 and 7, and the lower solid line in Fig. 8 represent the theoretical Sn/O surface atomic ratio based on 100% distribution of the Sn throughout the alumina lattice (solid solution). Any deviation of the measured XPS Sn/O ratio from this line indicates a surface excess (or deficit) of tin.

In Fig. 6, large positive deviations of the Sn/O ratio occur for the aqueous impregnations, with the curve exhibiting a maximum near 3wt%. The shape of the curve is uncertain in Fig. 6(a) due to data fluctuations. The main point is that a massive excess of Sn is observed over that expected for normal impregnation into the γ-Al_2O_3 pores (dashed line). After impregnation with Pt the distribution improves and the surface Sn/O ratio is closer to the dashed line. For the acetone case (Fig. 7) there is little difference in the Sn/O ratios before and after impregnation with Pt, although the curve still deviates strongly from the uniform distribution line in a similar fashion to the Pt–Sn results of Fig. 6.

In Fig. 8 is shown all the data for Sn/O ratios of the Pt–Sn catalysts, including three extra points; 1 and 2 are coprecipitated (Patent) preparations and point 3 is an acetone impregnation of the complex $[Pt(SnCl_3)_2Cl_2][Et_4N]_2$. It is clear that all of the impregnated catalysts fall on a curve in Fig. 8, which deviates strongly from the uniform

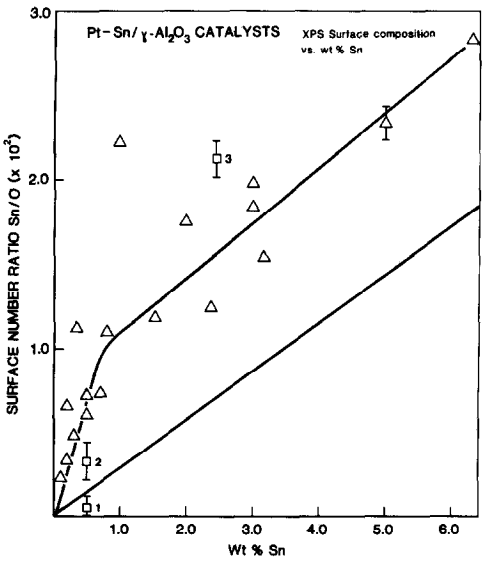

FIG. 8. All data for Pt–Sn/γ-Al_2O_3 catalysts plotted as a surface vs bulk composition graph. Points 1, 2 are coprecipitated catalysts (0.5% Pt) and point 3 is the Pt–Sn complex in Fig. 5. Note the significant surface excess of Sn in all impregnated catalysts compared with the coprecipitated ones.

distribution line in the first 0.8 wt% or so then runs parallel to it up to 6 wt%. By contrast, the coprecipitated (Patent) preparations both lie much closer to the uniform distribution line in Fig. 8. This data may be explained by a simple model. During the initial impregnations, Sn ions adsorb strongly on the alumina outer surface with poor penetration into the internal surface. Impregnation with Pt redistributes the tin somewhat but the tin remains in excess at the external surface (top 50 Å or so) than in the pores of the alumina. As the loading increases beyond 0.8 wt% the external surface begins to saturate with Sn and further penetration into the pores of the Al_2O_3 occurs. In the case of the coprecipitated catalysts, tin is already dispersed throughout the alumina matrix and one obtains a Sn/O surface ratio which is close to the expected value. Even in the case of the Pt–Sn complex in Fig. 8 a surface excess of Sn (by a factor of 2) is obtained with the standard impregnation process.

Without discussing the results in detail here, it should be clear from Fig. 8 that there is a strong adsorption of Sn(II,IV) on the alumina external surface causing a buildup of tin in the early stages of impregnation. Even calcining the catalysts is not sufficient to redistribute the tin. It appears that, of the catalysts studied, the coprecipitated tin–alumina preparations give the best distribution of tin in the alumina particles and circumvent the strong adsorption problem encountered with impregnation methods.

3. *XRD Results for Pt–Sn/γAl_2O_3 Catalysts*

In the majority of cases, there was no XRD evidence for the presence of metallic tin or a Pt–Sn alloy. XRD showed no lines attributable to a new Pt–Sn, or Sn phase. The exceptions were several of the water-based impregnations with a high tin loading which were not impregnated with platinum (upper curve, Fig. 6). After reduction at 500°C some metallic tin was detected on these tin-only catalysts, and electron microscopy confirmed that a separate tin oxide phase with some tin globules was present on the alumina after the reduction at 500°C. The formation of metallic tin on these samples was most likely a result of reduction of the tin oxide phase. On all of the other catalysts, however, no other phases could be seen with electron microscopy or XRD. In both the XRD and electron microscopy, however, air exposure was necessary before examining the reduced catalysts.

4. *Silica-Supported Pt–Sn Catalysts*

We prepared four different Pt,Sn/SiO_2 catalysts all with 0.5% Pt and tin loadings ranging from 0.14 to 1.0% Sn. The TPR results indicated that the percentage tin reduction (Sn(IV) to Sn(0)) varied from 30 to 55% based on complete reduction of Pt(IV) to Pt(0). Similarly we observed a metallic tin component in the Sn 3d XPS spectra after reduction. Estimates of the percentage reduction to the metallic state (Sn(0)) based on the XPS areas varied between 25 and 48%. In most cases XRD was unable to detect the presence of any Pt–Sn alloy phases with the exception of some catalysts which were calcined prior to reduction at 500°C. One example was a 1% Sn,0.5% Pt catalyst calcined for 24 h at 500°C prior to reduction. XRD revealed the presence of some Pt–Sn (niggliite) phase. These silica results confirm that platinum–tin alloys may form on a silica support in contrast to γ-Al_2O_3.

5. *Reaction Data: The Effect of Tin on the Reactions of Methylcyclopentane (MCP) and Cyclohexane (CH)*

The reaction data (activities and product distribution) are summarized in Table 1. The activity for the dehydrogenation of cyclohexane at 600 K versus tin content of the catalysts is shown in Fig. 9. Very small tin additions had a negligible effect on the dehydrogenation rate, but further additions significantly reduced the rate, with lesser

TABLE 1

Reactions of Methylcyclopentane (MCP) and Cyclohexane (CH)

Catalyst	Metal content (wt%)		MCP Reaction (670 K)				CH-dehydrogenation[c] conversion (%)		
			Product distribution (mol%)			Conversion (%)			
	Pt	Sn	Hexanes[a]	Benzene	MCP		600 K	670 K	
1	0.5	—	78.0	2.3	16.8[b]	22.0	92	100	Initial
			63.8	3.8	30.8[b]	12.5	—	—	Steady state
2 (Acetone)	0.5	0.3	79.0	3.0	16.0[b]	21.5	92	100	Initial
			62.0	5.5	31.0[b]	12.5	—	—	Steady state
3 (Aqua regia)	0.5	0.7	65.1	8.0	27.1	19.5	65	100	Initial
			46.0	12.3	41.7	12.0	—	—	Steady state
4 (Acetone)	0.5	1.6	40.7	13.0	46.3	16.4	32	100	Initial
			24.0	20.0	56.0	11.3	—	—	Steady state
5 (Acetone)	0.5	2.4	12.5	20.5	67.0	7.0	15	60	Initial
			8.5	22.0	69.0	6.2	—	—	Steady state
6 (Acetone) (Aqua regia)	0.5	3.2	11.6	6.0	82.4	6.1	12	50	Initial
			8.0	6.5	85.5	5.8	—	—	Steady state
7 (Coprecip)	0.5	0.5	18.2	11.1	70.7	8.2	35	100	Initial
			12.4	13.5	74.1	7.7	—	—	Steady state
8 (From $[Et_4N_2]_2[Pt-(SnCl_3)_2Cl_2]$)	2.0	2.4	2.0	6.0	92.0	4.5	2	9[d]	Initial
			—	—	—	—	—	—	Steady state

Note. Catalyst 0.15 g, HC to H_2 ratio, 1 to 8; flow rate 40 cc min^{-1}.

[a] Consist of 2MP, 3MP, and *n*-hexane.

[b] Some products $<C_5$ formed.

[c] No deactivation with time on stream for CH dehydrogenation.

[d] Cyclohexene formed: 20 mol%.

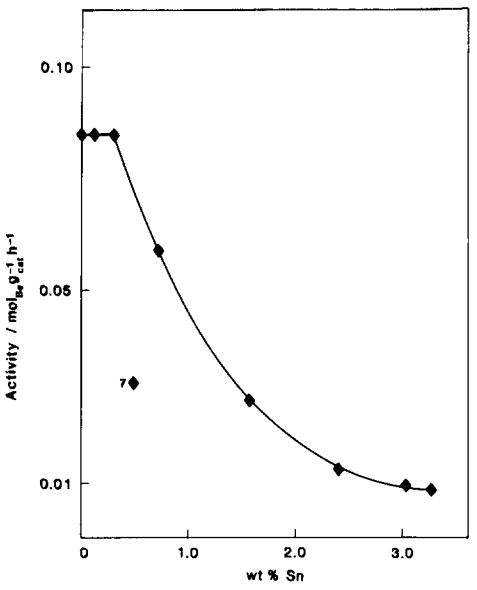

FIG. 9. Dehydrogenation of cyclohexane at 600 K as a function of tin content. The point marked with No. 7 represents the coprecipitated catalyst.

effects at higher loadings (>2% Sn). The coprecipitated catalyst deviated from this relationship and exhibited a (CH) conversion significantly lower than expected for a catalyst containing 0.5% Sn. Benzene is the sole reaction product from cyclohexane conversion on most catalysts at 600 K but small amounts of cyclohexenes were obtained on the highest tin loading (3% Sn) and also on catalyst 8 prepared from the Pt–Sn complex $[Pt(SnCl_3)_2Cl_2][Et_4N]_2$. This latter catalyst had a very low conversion for cyclohexane at 600 K and produced up to 25 mole% cyclohexenes.

Activities for methylcyclopentane conversion (initial and steady state activities) also decrease with increasing tin content. Figure 10 shows a steady activity loss up to 1.5 wt% Sn followed by a sharp activity drop in the region 1.5 to 2.5 wt% Sn. Increasing the tin content further had little effect on the MCP conversion. The difference between the initial and steady state activities is a measure of the catalyst deactivation with time on stream. The difference is largest for the pure Pt catalyst and diminishes rapidly above 1.5 wt% Sn, in agreement with previous studies (*1, 9*) where tin additions were found to reduce catalyst deactivation rates.

The presence of tin also dramatically alters the catalyst selectivity in MCP conversion. A plot of the product distribution versus tin content of the catalysts (Fig. 11) shows a strong decline in the production of open-chain hexanes (2-methylpentane, 3-methylpentane, and *n*-hexane) with increasing tin content. Benzene production passes through a maximum at 1.5 to 2.5 wt% Sn and the amount of methylcyclopentenes among the reaction products increases with tin content. On the basis of the MCP product distributions, catalyst 7 (coprecipitated catalyst), containing 0.5% Sn displayed a reaction behavior characteristic of an impregnated catalyst with a tin loading >2.0 wt%. For catalyst 8, prepared with a Pt–Sn complex, a high selectivity toward formation of methylcyclopentenes was found, in agreement with previous work (*10*).

The results in Table 1 are in essential agreement with published work on the effects of tin on hydrocarbon reaction selec-

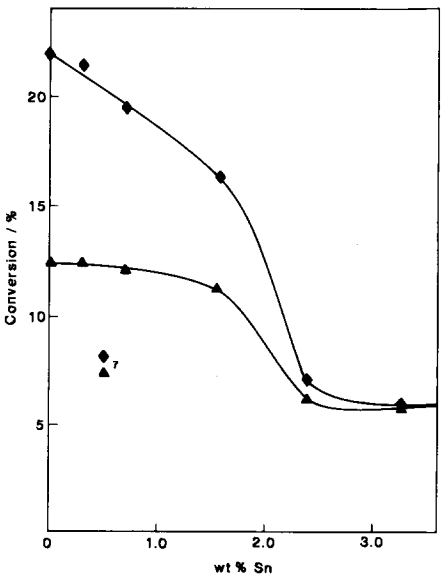

FIG. 10. Plot of initial (◇) and steady state (△) activities for MCP conversion versus tin content. The coprecipitated catalyst is marked as No. 7.

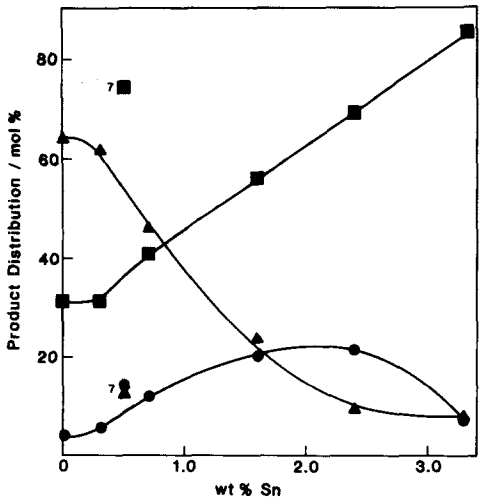

FIG. 11. Product distribution (steady state conversion) from the conversion of MCP as a function of tin content. (△) Hexanes (2MP, 3MP, N–H); (○) benzene; (□) methylcyclopentenes. The points marked with a No. 7 represent the coprecipitated catalyst.

tivity and activity on Pt–Sn catalysts. Our results show, however, that low loadings of tin (below 1 wt% Sn) have relatively little effect on the reactions and above 1.5 wt% Sn very significant changes have occurred. We believe that the insensitivity to the presence of tin at low loadings is a direct consequence of the inhomogeneous distribution of tin with respect to platinum in this particular set of catalysts. For the coprecipitated and Pt–Sn complex catalysts (7 and 8 in Table 1) tin has a profound effect on the reaction behavior.

Dautzenberg *et al.* (*2*) have already established that the method of tin introduction has a marked effect on the catalyst properties. They tested catalysts where the tin was added after Pt deposition and prior to Pt deposition. At low tin contents, impregnation of tin prior to platinum deposition did not lead to a modified catalyst performance. A comparison of Fig. 9 with data by Völter *et al.* (*9*) indicates that their catalysts were affected to a much stronger extent by low loadings of tin than our impregnated catalyst: 0.3 wt% Sn in Völter's (*9*) catalyst caused the dehydrogenation rate for cyclohexane to drop to 50% of the pure Pt value. For 0.8 wt% Sn, Völter's catalysts had a dehydrogenation rate an order of magnitude lower. The equivalent effects were observed with our impregnated catalysts for tin contents of 1 and 3 wt%, respectively. Only the coprecipitated catalyst agrees closely with Völter's study. It is significant to note that the latter authors prepared their catalysts via a coimpregnation of H_2PtCl_6 and $SnCl_2$, which is different to the sequential method used in the present study.

The discrepancies between our results and other work can be explained by a model of the tin and platinum distribution in this series of catalysts. According to the XPS results, only the coprecipitated catalyst contained a uniform distribution of tin throughout the alumina matrix, based on the expected surface intensity of Sn/O in the XPS data. Impregnated catalysts, on the other hand, whether impregnated from water or acetone solutions all displayed a strong enrichment of tin on the alumina external surface. Significant penetration into the internal surface (pores) seemed to occur only at tin contents >1 wt% as the slope of the curve in Fig. 8 became the same as the theoretical line. Assuming a homogeneous platinum distribution throughout the alumina, the tin and platinum must therefore be physically separated in the catalyst at low impregnated tin loadings, but begin to come in contact at higher loadings. For the coprecipitated case both the XPS and reaction results support a model where the tin and platinum are both uniformly distributed throughout the matrix. In the case of the impregnated Pt–Sn complex, the XPS results showed an excess of tin on the external surface (Fig. 8) but the reactivity was characteristic of a close interaction between Pt and Sn. It is most likely that the strong adsorption of the complexes on alumina results in both Pt and Sn being in excess at the external surface.

Apart from the obvious differences in distribution of Sn and Pt in the different

catalysts, our XPS results showed that the lowest oxidation state of tin was Sn(II) and we therefore found no evidence to support the "alloy hypothesis" of Dautzenberg *et al.* (*2*).

Preparations of platinum–tin catalysts are therefore strongly affected by the apparent affinity of tin ions for alumina, and impregnation methods seem to give variable results with a tendency for Pt to be uniformly distributed with tin in surface excess. Coprecipitation methods give a uniform tin distribution and Pt can then be easily distributed to come in intimate contact with the tin ions. Impregnated Pt–Sn complexes have a probable surface excess of both components but have substantially modified reaction behavior. It seems obvious from the present work that coprecipitated catalysts achieve the maximum contact between Pt and tin ions and have a uniform distribution of both species. Coprecipitation would seem to be the most efficient way of distributing tin in Pt–Sn catalysts.

Regarding the mechanism of modification of platinum reactivity by Sn(II) on γ-Al_2O_3 catalysts, two possibilities are the most likely. First, Sn(II) may act as an electronic modifier of the semiconducting properties of the alumina matrix in the vicinity of the platinum particles. Second, surface tin ions may be present on the platinum particles, although one might expect these to form a Pt–Sn alloy under hydrogen-reducing conditions. We believe that the strong affinity of Sn(II) for γ-Al_2O_3 and the lack of reduction supports the ideas presented by Burch (*1*), that Sn(II) is a surface modifier of γ-Al_2O_3 and the reactivity changes are most likely due to changes in the electronic interaction between Pt and Sn(II)–γ-Al_2O_3.

REFERENCES

1. Burch, R., *J. Catal.* **71,** 348, 360 (1981).
2. Dautzenberg, F. M., Helle, J. N., Biloen, P., and Sachtler, W. M. H., *J. Catal.* **63,** 119 (1980).
3. Muller, A. C., Engelhard, P. A., and Weisand, J. E., *J. Catal.* **56,** 65 (1979).
4. Bacaud, R., Bussiere, P., and Figueras, F., *J. Catal.* **69,** 399 (1981).
5. Bouwman, R., Toneman, L. H., and Holscher, A. A., *Surf. Sci.* **35,** 8 (1973).
6. Yermakov, Y. I., Kuznetsov, B. N., and Zakharov, V. A., "Catalysis by Supported Complexes," pp. 351–415. Elsevier, Amsterdam, 1981.
7. Kuznetsov, B. N., Duplyakin, V. K., Kovalchuk, V. I., Ryndin, Yu.A., and Belyi, A. S., *Kinet. Catal.* **22,** 1484 (1981).
8. Lau, C. L., and Wertheim, G. K., *J. Vac. Sci. Technol.* **15,** 622 (1978).
9. Völter, J., Lietz, G., Uhlehamann, M., and Hermann, M., *J. Catal.* **68,** 42 (1981).
10. Kuznetsov, B. N., Duplyakin, V. K., Kovalchuk, V. I., Ryndin, Y. A., and Belyi, A. S., *Kinet. Catal.* **24,** 1183 (1982).
11. Kerkhof, F. P. J. M., and Moulijn, J. A., *J. Phys. Chem.* **83,** 1612 (1979).